Enhancing the energy storage capacity of a symmetric supercapacitor employing α-$Cu_2P_2O_7$ produced by a template-based co-precipitation approach.

Jay B. Patel[1-3], Karan S. Modi[1,3], Pruthvi Patel[1,3], Dharti Patel[1,3], Vanaraj Solanki[3], Bhavin Patel[4], Mitesh H. Patel*[2,3]

[1]*P. D. Patel Institute of Applied Sciences, Charotar University of Science and Technology, Changa, Anand District, Gujarat 388421, India*

[2]*Analube Lab, Pramukh Swami Centre of Excellence for Renewable Energy, Charotar University of Science and Technology, Changa, Anand District, Gujarat 388421, India*

[3]*Dr. K. C. Patel Research and Development Centre, Charotar University of Science and Technology, Changa, Anand District, Gujarat 388421, India*

[4]*Natubhai V. Patel college of Pure and applied science, CVM* University, *Vallabh Vidhyanagar, Anand District, Gujarat 388120, India*

**Corresponding author:* Email: miteshpatel.bio@charusat.ac.in

1. XRD analysis of α-$Cu_2P_2O_7$ electrode

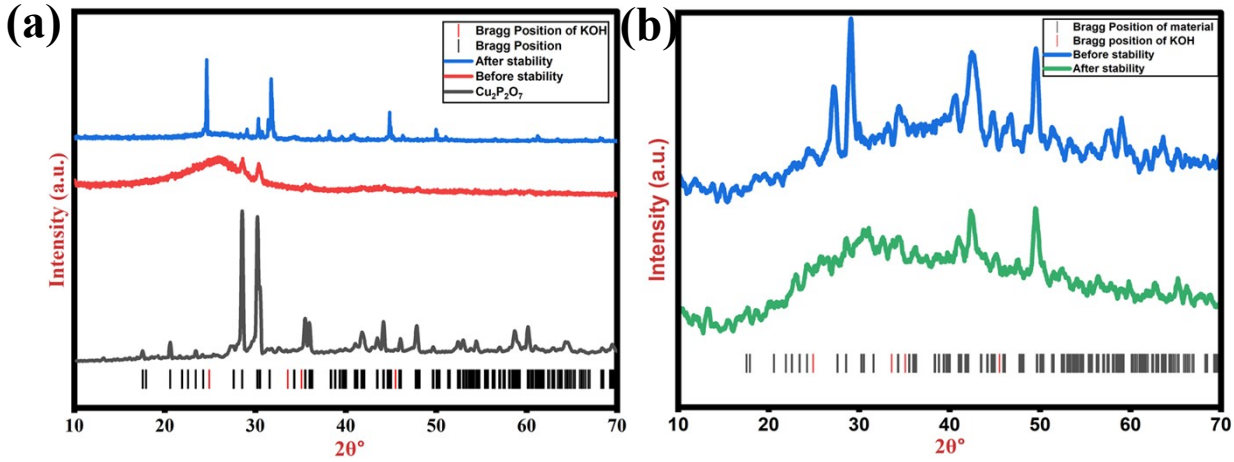

Figure S 1 (a) XRD patterns of α-$Cu_2P_2O_7$ electrode, before and after 5000 cycles, (b) XRD patterns of Symmetric SCs α-$Cu_2P_2O_7$ electrodes, before and after 10000 cycles.

Figure S1(a) shows the X-ray diffraction (XRD) patterns of the α-$Cu_2P_2O_7$ electrode, recorded before and after 5000 charge-discharge cycles in a three-electrode system. XRD analysis of the α-$Cu_2P_2O_7$ electrode after 5000 cycles reveals two more KOH peaks at 2θ angles of 24.9°, 33.6°, 34.6°, and 44.8°. These peaks are caused by KOH residue on the surface of carbon cloth (CC) fibers. All other peaks correspond to the conventional Bragg position, confirming the material's stability across 5000 charge-discharge cycles.

X-ray diffraction analysis (Figure S1(b)) was carried out on the electrode material before and after 10000 charge-discharge cycles. The pristine electrode's pattern validates the material's initial phase purity. However, the used electrode's XRD pattern shows extra diffraction peaks in addition to the original α-$Cu_2P_2O_7$ reflections. The identified new peaks

correspond to KOH and carbon nano tubes. The presence of KOH residue on the SS electrode's surface causes the formation of a new peak. Similarly, the emergence of activated carbon is the result of extended cycling of the electrode material.

3. FE-SEM and EDX of before and after cycling stability of electrode

3.1. Before cycling stability

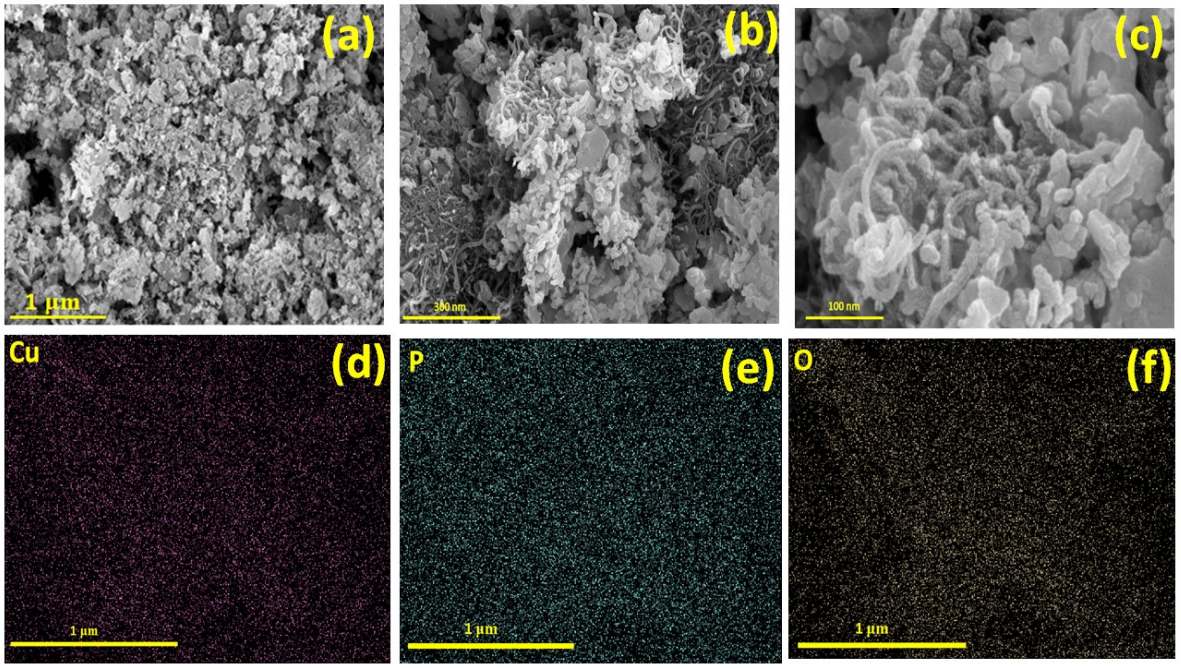

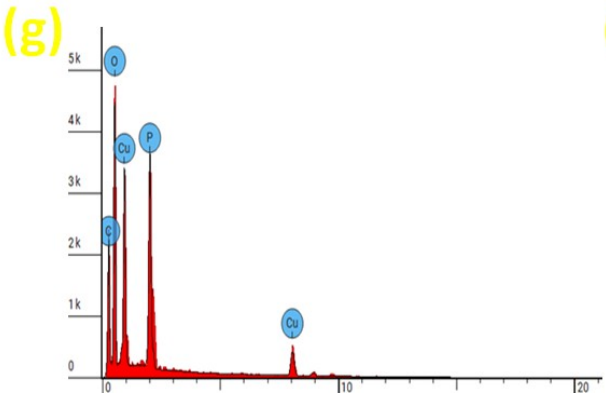

(h)

Element Symbol	Atomic Concentration [%]	Weight Concentration [%]
C	42.38	26.40
O	39.53	32.80
P	11.14	17.90
Cu	6.95	22.90

Figure S2. (a-c) FE-SEM image of before cycling stability and (d-g) Elemental mapping (h) Table of concentration

To validate the structural and morphological stability of the α-$Cu_2P_2O_7$ electrode during long-term electrochemical cycling, FE-SEM characterization and EDX elemental analysis were performed on the electrode after 5000 charge-discharge cycles (Figure S2). Figure S2(a–c) presents FE-SEM images of the α-$Cu_2P_2O_7$ electrode before cycling at different

magnifications (1 µm, 300 nm, and 100 nm scale bars), revealing an interconnected porous morphology with a rough surface arising from the irregular polygonal nanoflake architecture of the active material uniformly distributed on the current collector. The EDX spectrum [Figure S2(g)] and elemental table [Figure S2(h)] confirm the presence of C (42.38 %), O (39.53%), P (11.14 %), and Cu (6.95%), where the high carbon content is attributed to the MWCNT conducting agent used during electrode fabrication. The uniform elemental mapping [Figure S2(d–f)] confirms the homogeneous distribution of Cu, P, and O across the electrode surface prior to cycling.

3.2 After cycling stability

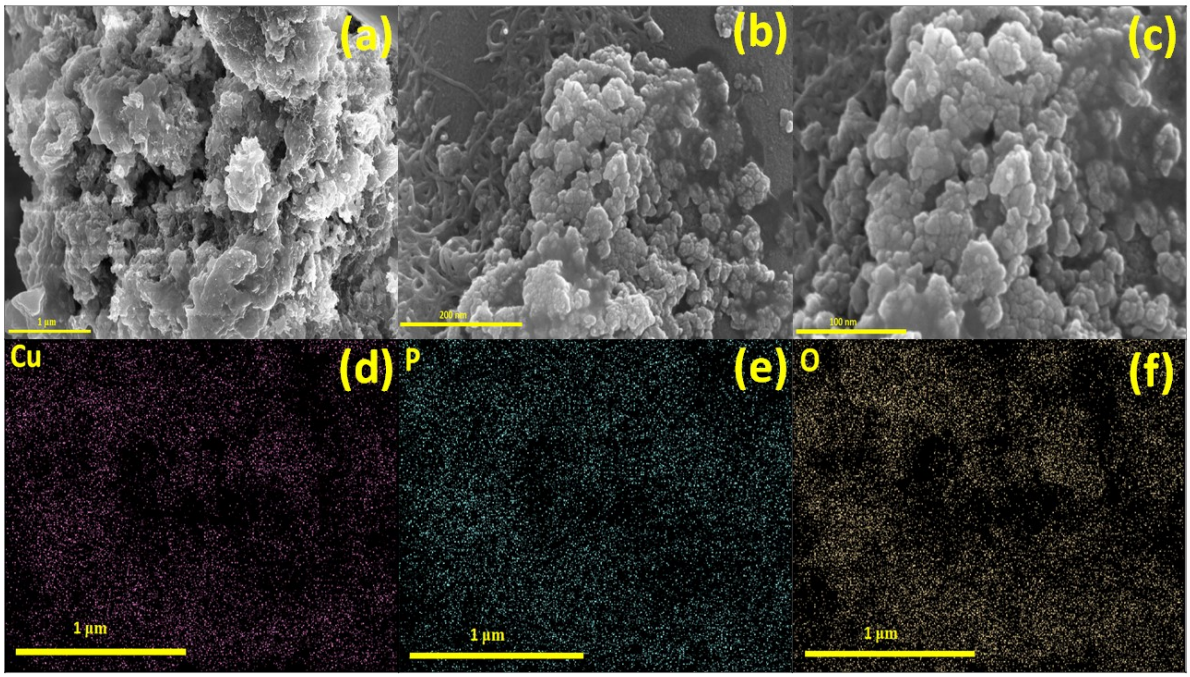

(g)

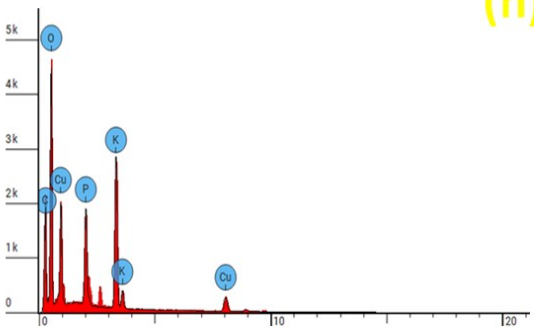

(h)

Element Symbol	Atomic Concentration [%]	Weight Concwntration [%]
C	22.29	12.60
O	54.31	40.90
P	5.83	8.50
K	12.66	23.30
Cu	4.92	14.70

Figure S3. (a-c) FE-SEM image of after cycling stability and (d-g) Elemental mapping (h) Table of concentration

As illustrated in Figure S3(a–c), the interconnected porous morphology of the α-$Cu_2P_2O_7$ electrode is largely preserved after prolonged cycling, with no visible cracking, pulverization, or delamination of the active material from the current collector. This morphological stability is consistent with the 90% capacitance retention observed after 5000 cycles and confirms the mechanical robustness of the synthesized material. EDX analysis of the cycled electrode [Figure S3(g,h)] reveals the continued presence of Cu and P, confirming that no significant leaching or phase decomposition of α-$Cu_2P_2O_7$ occurred during cycling. The appearance of a K peak (12.66%) after cycling is attributed to the residual adsorption of K^+ ions from the 6 M KOH electrolyte onto the electrode surface, which is an expected phenomenon for KOH-based supercapacitor systems and does not indicate structural degradation. The slight increase in O content (from 39.53% to 54.31%) is similarly attributed to surface-adsorbed KOH species. The elemental mapping [Figure S3(d–f)] confirms the uniform distribution of Cu, P, and O elements across the electrode surface after cycling, further supporting the compositional integrity of α-$Cu_2P_2O_7$. Collectively, the post-cycling FE-SEM and EDX characterization provide direct morphological and compositional evidence for the outstanding long-term stability of α-$Cu_2P_2O_7$ as a symmetric supercapacitor electrode material.

4. Cyclic voltammetry of α-$Cu_2P_2O_7$ material at different potential

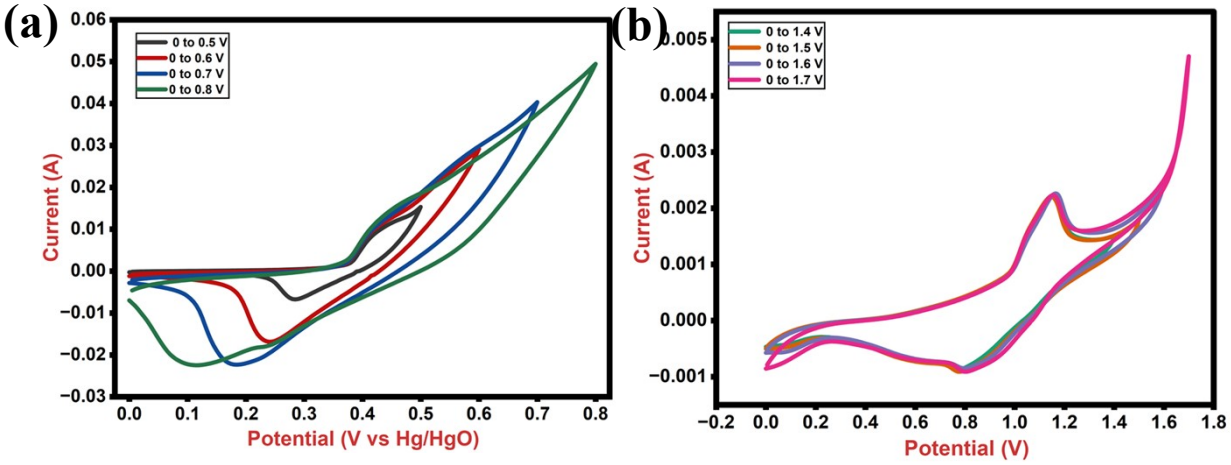

Figure S (4) CV for three electrode configurations at different potential of α-$Cu_2P_2O_7$

Figure S(4 (a)) demonstrates the CV of the α-$Cu_2P_2O_7$ electrode taken in different potential windows and a fixed scan rate of 20 mV/s. The data reveal that the electrode has a stable working window between 0 to 0.6 V in 6M aqueous KOH electrolyte. The performance of the electrode material is further limited by electrochemical polarization as the potential window increases.

Figure S(4 (b)) replicate the CV of symmetric supercapacitor device electrode, took at various potential with fixed scan rate of 20 mV/s.

5. The below data of Crystallographic information file (CIF) from the Rietveld refinement.

##
###

FullProf-generated CIF output file (version: May 2019)

Template of CIF submission form for structure report

##
###

 # This file has been generated using FullProf.2k taking one example of

 # structure report provided by Acta Cryst. It is given as a 'template' with

 # filled structural items. Many other items are left unfilled and it is the

 # responsibility of the user to properly fill or suppress them. In principle

 # numerical value depending on the kind of CIF item.

 # See the document: cif_core.dic (URL: http://www.iucr.org) for details.

 # Please notify any error or suggestion to:

 # Juan Rodriguez-Carvajal (jrc@ill.eu)

 # Improvements will be progressively added as needed.

 # Date: 11/12/2024 Time: 13:37:04.714

_audit_creation_date 11/12/2024

_audit_creation_method "FullProf Suite"

 # PROCESSING SUMMARY (IUCr Office Use Only)

_publ_requested_category ? # Acta C: one of CI/CM/CO/FI/FM/FO

 # Definition of non standard CIF items (Reliability indices used in FULLPROF)

 # Name Explanation Standard?

 # ------ ---------- ---------

'_pd_proc_ls_prof_cR_factor' 'Prof. R-factor CORRECTED for background' no

'_pd_proc_ls_prof_cwR_factor' 'wProf.R-factor CORRECTED for background' no

'_pd_proc_ls_prof_cwR_expected' 'wProf.Expected CORRECTED for background' no

'_pd_proc_ls_prof_chi2' 'Chi-square for all considered points' no

'_pd_proc_ls_prof_echi2' 'Chi-2 for points with Bragg contribution' no

#==========

 # 3. TITLE AND AUTHOR LIST

_publ_section_title

; ' #$Date: 2017-07-04 18:48:19 +0300 (Tue, 04 Jul 2017) $'

;

_publ_section_title_footnote

 # The loop structure below should contain the names and addresses of all

 # authors, in the required order of publication. Repeat as necessary.

_atom_type_scat_source

cu 13.33800 3.58280 7.16760 0.24700 5.61580 11.39660

1.67350 64.81260 1.19100 -2.01900 0.58900

International_Tables_for_Crystallography_Vol.C(1991)_Tables_6.1.1.4_and_6.1.1.5

p 6.43450 1.90670 4.17910 27.15700 1.78000 0.52600

1.49080 68.16450 1.11490 0.28300 0.43400

International_Tables_for_Crystallography_Vol.C(1991)_Tables_6.1.1.4_and_6.1.1.5

o 3.04850 13.27710 2.28680 5.70110 1.54630 0.32390

0.86700 32.90890 0.25080 0.04700 0.03200

International_Tables_for_Crystallography_Vol.C(1991)_Tables_6.1.1.4_and_6.1.1.5

#==========

==========

 # 6. POWDER SPECIMEN AND CRYSTAL DATA

_symmetry_cell_setting Monoclinic

_symmetry_space_group_name_H-M 'C 1 2/c 1'

_symmetry_space_group_name_Hall '-C 2yc'

_symmetry_equiv_pos_as_xyz

'x,y,z'

'-x,y,-z+1/2'

'-x,-y,-z'

'x,-y,z+1/2'

'x+1/2,y+1/2,z'

'-x+1/2,y+1/2,-z+1/2'

'-x+1/2,-y+1/2,-z'

'x+1/2,-y+1/2,z+1/2'

_cell_length_a 6.84409

_cell_length_b 8.11770

_cell_length_c 9.13991

_cell_angle_alpha 90.0000

_cell_angle_beta 109.210

_cell_angle_gamma 90.0000

_cell_volume 479.524

_cell_formula_units_Z ?

_cell_measurement_temperature ?

_cell_special_details

; ?

;

 # The next three fields give the specimen dimensions in mm. The equatorial

 # plane contains the incident and diffracted beam.

_pd_spec_size_axial ? # perpendicular to

 # equatorial plane

_pd_spec_size_equat ? # parallel to

 # scattering vector

 # in transmission

_pd_spec_size_thick ? # parallel to

 # scattering vector

 # in reflection

 # The next five fields are character fields that describe the specimen.

_pd_spec_mounting # This field should be

 # used to give details of the

 # container.

; ?

;

_pd_spec_mount_mode ? # options are 'reflection'

 # or 'transmission'

_pd_spec_shape ? # options are 'cylinder'

 # 'flat_sheet' or 'irregular'

_pd_char_particle_morphology ?

_pd_char_colour ? # use ICDD colour descriptions

 # The following three fields describe the preparation of the specimen.

 # The cooling rate is in K/min. The pressure at which the sample was

 # prepared is in kPa. The temperature of preparation is in K.

 # 7. EXPERIMENTAL DATA

_exptl_special_details

; ?

;

 # The following item is used to identify the equipment used to record

 # the powder pattern when the diffractogram was measured at a laboratory

 # other than the authors' home institution, e.g. when neutron or synchrotron

 # radiation is used.

_pd_instr_location

; ?

;

_pd_calibration_special_details # description of the method used

 # to calibrate the instrument

; ?

;

_diffrn_ambient_temperature ?

_diffrn_source ? # Put here: 'rotating-anode X-ray tube' or similar

_diffrn_radiation_type 'X-ray'

_diffrn_source_target ? # Put here the chemical symbol of the anode

_diffrn_detector_type ? # make or model of detector

_pd_meas_scan_method ? # options are 'step', 'cont',

 # 'tof', 'fixed' or

 # 'disp' (= dispersive)

 _# The following four items give details of the measured (not processed)

 # powder pattern. Angles are in degrees.

_pd_meas_number_of_points 3006

_pd_meas_2theta_range_min 10.12340

_pd_meas_2theta_range_max 70.97740

_pd_meas_2theta_range_inc 0.020256

#==========

==========

 # 8. REFINEMENT DATA

_refine_special_details

; ?

;

 # Use the next field to give any special details about the fitting of the

 # powder pattern.

_pd_proc_ls_special_details

; ?

;

 # The next three items are given as text.

 # The following profile R-factors are NOT CORRECTED for background

 # The sum is extended to all non-excluded points.

 # These are the current CIF standard

_pd_proc_ls_prof_R_factor 4.6639

_pd_proc_ls_prof_wR_factor 6.6163

_pd_proc_ls_prof_wR_expected 5.1133

 # The following profile R-factors are CORRECTED for background

 # The sum is extended to all non-excluded points.

 # These items are not in the current CIF standard, but are defined above

_pd_proc_ls_prof_cR_factor 26.9940

_pd_proc_ls_prof_cwR_factor 23.3414

_pd_proc_ls_prof_cwR_expected 18.0388

 # The following items are not in the CIF standard, but are defined above

_pd_proc_ls_prof_chi2 1.6743

_pd_proc_ls_prof_echi2 1.8189

 # Items related to LS refinement

_refine_ls_R_I_factor 11.4205

_refine_ls_number_reflns 259

_refine_ls_number_parameters 2

_refine_ls_number_restraints 0

 # The following four items apply to angular dispersive measurements.

 # 2theta minimum, maximum and increment (in degrees) are for the

 # intensities used in the refinement.

_pd_proc_2theta_range_min 10.2331

_pd_proc_2theta_range_max 71.0871

_pd_proc_2theta_range_inc 0.020256

_pd_proc_wavelength 1.540560

_pd_block_diffractogram_id ? # The id used for the block containing

 # the powder pattern profile (section 11)

 # Give appropriate details in the next two text fields.

_pd_proc_info_excluded_regions ?

_pd_proc_info_data_reduction ?

 # The following items are used to identify the programs used.

__computing_structure_refinement FULLPROF

_computing_molecular_graphics ?

_computing_publication_material ?

#==========

 # 9. ATOMIC COORDINATES AND DISPLACEMENT PARAMETERS

loop_

_atom_site_label

_atom_site_fract_x

_atom_site_fract_y

_atom_site_fract_z

_atom_site_U_iso_or_equiv

_atom_site_occupancy

_atom_site_adp_type

_atom_site_type_symbol

Cu3 -0.0078 0.31228 0.50805 -0.0186 1.00000 Uiso Cu

P31 0.20039 -0.0038 0.20632 -0.0130 1.00000 Uiso P

O31 0.00000 0.04557 0.25000 -0.0161 1.00000 Uiso O

O32 0.38042 0.01015 0.35155 -0.0198 1.00000 Uiso O

O33 0.16824 0.15064 0.11162 -0.0121 1.00000 Uiso O

O34 0.21913 -0.1504 0.11964 -0.0372 1.00000 Uiso O

 # Note: if the displacement parameters were refined anisotropically

 # the U matrices should be given as for single-crystal studies.

#==========

 # 10. DISTANCES AND ANGLES / MOLECULAR GEOMETRY

_geom_special_details ?

loop_

_geom_bond_atom_site_label_1

_geom_bond_atom_site_label_2

_geom_bond_site_symmetry_1

_geom_bond_site_symmetry_2

_geom_bond_distance

_geom_bond_publ_flag

? ? ? ? ? ?